Two-dimensional photonic-crystal vertical-cavity array for nonlinear optical image processing

Daniel F. Sievenpiper, Cedric F. Lam, and Eli Yablonovitch

We investigate the electromagnetic properties of a two-dimensional (2-D) photonic-crystal array of vertical cavities for use in nonlinear optical image processing. We determine the 2-D photonic band structure of the array, and we discuss how it is influenced by the degree of interaction between cavities. We study the properties of defects in the 2-D lattice and show that neighboring cavities interact through their overlapping wave functions. This interaction can be used to produce nearest-neighbor nonlinear Boolean functions such as AND, OR, and XOR, which are useful for optical image processing. We demonstrate the use of 2-D photonic bandgap structures for image processing by removing noise from a sample image with a nearest-neighbor AND function. © 1998 Optical Society of America

OCIS codes: 070.4340, 100.2000, 100.2550, 190.0190, 200.3760, 200.4690.

Most optical image-processing systems use linear elements such as lenses, gratings, and masks to perform transformations on images. These can be used to carry out many important functions, such as the Fourier transform of an image, the correlation of two images, various types of spatial filtering, and other linear operations.[1] Since these devices operate on an entire image at once, they exploit the inherently parallel nature of optical image-processing systems. However, many operations require nonlinear functions that cannot be achieved without a nonlinear device.[2] Such operations are often accomplished with a digital computer, in which the nonlinear elements are transistors. Unfortunately, this method requires the image to be processed pixel by pixel and lacks the speed and parallelism of an optical image-processing system.

We found that a two-dimensional (2-D) photonic-crystal[3–8] array of vertical cavities can be used to implement several nonlinear functions that are useful for optical image processing. The cavities interact with each other through their overlapping wave functions, resulting in coupling between neighbors. For defining an image on the array, some of the cavities are altered, causing a shift in their resonant frequencies. As a result of intercavity coupling, however, the magnitude of the frequency shift depends on not only the state of the cavity but also on the states of its neighbors. This effect is used to create nonlinear functions between neighboring cavities including AND, OR, and XOR (exclusive OR). We applied this idea to demonstrate a noise-removal process on a sample image by using a nearest-neighbor AND function.

Our experiments were performed in the microwave regime for simplicity, but one can extend the results to optical wavelengths by scaling the dimensions of the structure. The cavities consist of alternating layers of acrylic and polystyrene foam. The acrylic layers have an index of refraction of 1.6, and the polystyrene foam has an index of refraction roughly equal to unity. They are cut to a thickness of 0.32 and 0.52 cm, respectively, so that the thickness of each layer corresponds to one quarter of a wavelength at a frequency of 14.5 GHz. Ten periods of alternate layers are stacked to form a Bragg mirror. An additional quarter wavelength of foam is then inserted into the center of the stack to form a resonant cavity.

Our array is made up of a triangular lattice of these vertical cavities. We chose a triangular lattice since that is the most intuitively natural geometry in two dimensions; however, the square lattice of vertical cavities[6] also produces interesting results. Each cavity measures 3.81 cm from side to side and is hexagonally shaped to fill 2-D space perfectly. Foam spacers with a width of 0.3 cm are used to separate the cavities laterally. The entire array is held be-

The authors are with the Department of Electrical Engineering, University of California, Los Angeles, 64-144 Engineering IV, 405 Hilgard Avenue, Los Angeles, California 90095-1594.

Received 23 September 1997; revised manuscript received 1 December 1997.

0003-6935/98/112074-05$15.00/0

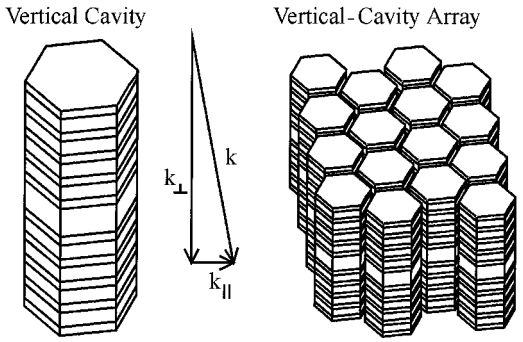

Fig. 1. Diagram of a single vertical cavity and a section of the array. The arrows indicate the large perpendicular component of the wave vector and the small parallel component in the plane of the array.

tween two acrylic support plates measuring 2.5 cm thick. Roughly 40 cavities make up our sample, a section of which is shown in Fig. 1.

Because of the lateral periodicity the array of cavities forms a 2-D photonic crystal. To determine the nature of the interaction between the cavities, we investigated the 2-D photonic band structure of our lattice. We performed measurements using a Hewlett-Packard Model 8720 network analyzer with horn antennas for transmitting and receiving. The structure was placed between the transmitting and receiving antennas and rotated with respect to the incoming waves. The waves had a large wave-vector component $k_\perp$ that was perpendicular to the plane of the lattice, as indicated by the arrows in Fig. 1. The rotation produced a small parallel component $k_\parallel$ that lay within the plane of the array. We constructed the 2-D photonic dispersion relation by measuring the resonant frequency of the cavities as a function of $k_\parallel$. In most research on 2-D photonic crystals the waves travel entirely in the plane of the 2-D lattice. Here the wave vectors were directed primarily perpendicular to the lattice with only a small parallel component, as in the research conducted by Birks *et al.*[7] on optical-fiber photonic crystals.

One can see the evolution of the band structure by measuring the dispersion relation with and without the foam spacers between the cavities. Without the spacers the cavities are packed tightly together. The structure exhibits a $1/\cos(\theta)$ relation between the resonant frequency and $k_\parallel$, as shown in the solid curves in Fig. 2. This can be regarded as the empty-lattice scenario. When small foam spacers are included between the cavities the frequencies are the same, except that gaps appear near the edges of the Brillouin zone. The gaps, centered around 15 GHz, separate the dispersion curve into energy bands, as indicated by the filled and open circles in Fig. 2. The width of the bands is a measure of the degree of interaction between the cavities, analogous to the overlap integral[9] in an atomic-crystal lattice. With 0.3-cm spaces between cavities the lowest band has a width of approximately 300 MHz.

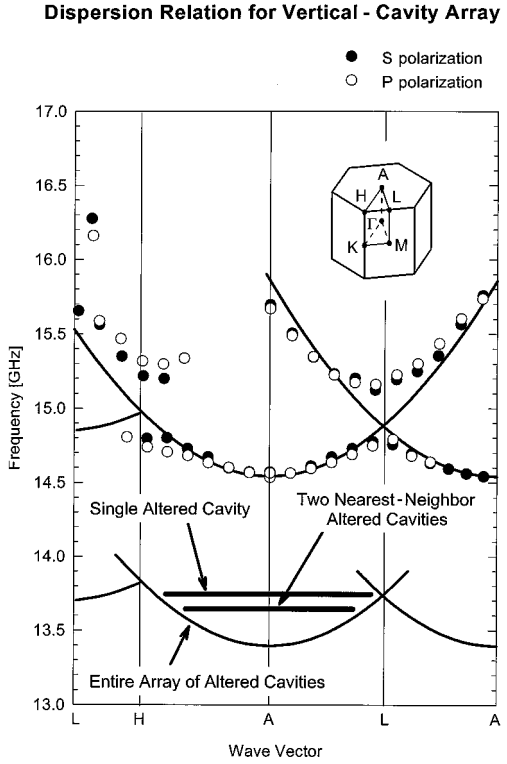

Fig. 2. Photonic band structure of the vertical-cavity array. The solid curves represent the structure without spaces between the cavities, as in the empty lattice model. The filled and open circles show measurements taken for s and p polarizations, respectively, when the cavities are spaced by 0.3 cm, producing gaps. The solid horizontal bars indicate the energy levels of a single frequency-shifted cavity and a pair of altered cavities within the array. The Brillouin zone is included for reference.

In a triangular lattice the electromagnetic interaction between the cavities is particularly complicated. For example, a triangular lattice exhibits frustration[10], which is absent in a square lattice. Frustration occurs when geometry forbids each lattice point from becoming polarized opposite to all its neighbors at the same time. Nonetheless, the nearly free-photon model can be used to determine the energy levels and corresponding electric fields at certain symmetry points in the Brillouin zone. At point L, for example, in the Brillouin zone inset in Fig. 2, the incident wave is coupled to an opposing wave that is reflected from the nearest point in the inverse lattice. The resulting standing waves form two energy levels corresponding to an air band and a dielectric band.[5] In real space the dielectric band includes states in which the peak electric field occurs in the center of the cavities, whereas in the air band the cavities sit on the nodes of the standing waves. Both s- and p-polarization states are possible, so each of these levels is doubly degenerate, and there is no mixing between polarization states.

At point H the situation is more interesting. In addition to the incident wave, there are two nearby points in the reciprocal lattice that contribute reflected waves. There are also two polarization

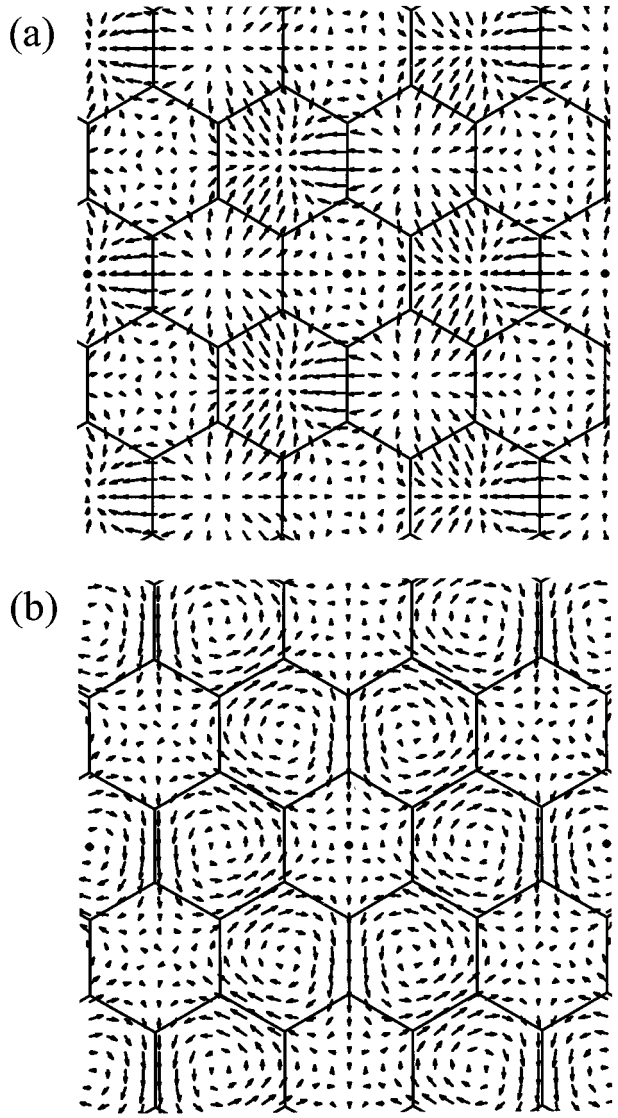

Fig. 3. (a) Highest energy level at point H on the top face of the Brillouin zone, composed entirely of p waves. The electric field produces a hedgehog pattern. (b) The lowest energy level composed entirely of s waves. The electric fields produce a swirl pattern.

states for a total of six interacting waves. Again, the nearly free-photon model can determine the relative amount of coupling between each wave. The various coupling constants form the basis of an eigenvalue problem that yields the energy levels and related electric field patterns. There are four energy levels at point H and the middle two are each doubly degenerate. The lowest is the swirl pattern shown in Fig. 3(a), which is entirely s-like. The highest is the p-like hedgehog pattern of Fig. 3(b). The four remaining modes associated with the two middle-energy levels have a mixture of both s and p characteristics. Experimentally the mixed nature of these states is confirmed by the observation of finite transmission peaks at point H that are seen when the transmitting and receiving antennas are cross polarized. Not all energy levels at point H are observed, but this may be because some modes do not couple well to free space.

Until now we have described the properties of a homogeneous array in which all the cavities are identical. To perform useful functions, however, we must introduce defects into the lattice, making some of the cavities different. We now describe the properties of such defects and their relation to the band-structure analysis given above. A defect is created by the alteration of the resonant frequency of one of the cavities. We do this by inserting an additional 0.16 cm of acrylic into the center of the cavity and removing an equal amount of foam to keep the overall layer spacing the same. This raises the effective index of refraction of the cavity and therefore lowers its resonant frequency. The frequency shift is sensitive to the exact location of the additional layer since the mode intensity varies along the length of the cavity. We place the additional layer of acrylic near the center of the cavity for maximum frequency shift. For the following experiments we also remove the foam spacers from between the cavities to maximize the degree of interaction.

If one cavity is altered and the rest of the array is left unchanged, that cavity experiences a frequency shift of approximately 750 MHz, indicated in Fig. 2 by the upper solid horizontal bar. The length of the bar is meant to show that the localized state takes up a large area of k space. Since the frequency shift is much larger than the width of the lowest energy band, we can conclude that the state is well localized to the altered cavity. If two neighboring cavities are altered, however, the pair will experience a greater frequency shift of approximately 850 MHz, indicated in Fig. 2 by the slightly lower horizontal bar. Thus two altered cavities next to each other will have a different resonant frequency than either one would have by itself. If all the cavities in the structure are altered, the resonant frequency of the array shifts downward by 1.1 GHz. In this case the entire band structure is shifted downward, indicated by the lower set of solid curves in Fig. 2.

We found that the resonant frequency of a particular cavity depends on its surroundings. This is because the mode of each cavity extends slightly into adjacent cavities, resulting in a coupling between nearest neighbors. In general, if two identical resonators are allowed to interact, they generate two new frequencies, one higher and one lower, centered around the original frequency of the resonators. This effect is seen in many examples, such as the bonding and antibonding modes of diatomic molecules or in metallic photonic bandgap structures with two interacting defects.[8] In the case of coupled vertical cavities the interaction generates a low-frequency symmetric mode and a higher-frequency antisymmetric mode. We detect only the symmetric mode, however, because we are illuminating the structure at normal incidence. Thus the interaction manifests itself as a downward frequency shift, causing two adjacent altered cavities to resonate at a lower frequency than one isolated altered cavity.

This interaction between neighboring cavities can be used to perform several important nonlinear image-processing functions. If a single isolated cavity is altered it resonates at a certain frequency, but if one of its neighbors is also altered both cavities resonate at a slightly lower frequency owing to their interaction. If we measure the transmission at this lower frequency, we obtain the AND function between the two cavities. Both neighboring cavities must be altered to detect transmission at the proper frequency. This could be accomplished with a narrow-band filter that selects for the two-cavity resonance. We can also produce the XOR function by using a different filter with a passband at the single-cavity resonance. In this way we detect only transmission if one isolated cavity is altered but none of its neighbors. Furthermore, if we use a filter with a wide passband that includes both frequencies we generate the OR function. We would then detect transmission either if an isolated cavity is altered or if two neighboring cavities are altered. These functions are slightly different from the usual Boolean functions of the same names because they are carried out in a 2-D lattice. Each operation is actually a function of the state of each cavity and all six of its nearest neighbors.

The results described above can be used to produce important optical image-processing functions. We demonstrate this by using the nearest-neighbor AND function to remove noise from a sample image. Fig. 4(a) shows an image of the number 7 with some pepper noise added in the form of two erroneous black pixels. Pepper noise appears as black spots on a white background, as opposed to salt noise, which is white spots on a black background.[11] The black shading in Fig. 4(a) denotes which pixels have had their resonant frequencies lowered in our vertical-cavity array. We measured the transmission spectrum of each cavity by placing the receiving horn against the acrylic support plate on the front of our structure. Figure 4(b) shows the results of transmission measurements at the frequency corresponding to altered pixels with several nearest neighbors altered. This criterion applies to most of the pixels in the number 7 but not the noise pixels, because they are isolated. Black shading is used in Fig. 4(b) to denote the pixels with transmission greater than -12 dB within the selected frequency range. Note that the single, isolated, altered cavities do not appear because they resonate at a slightly higher frequency. We effectively removed the pepper noise from the image by using the electromagnetic interaction between the cavities. Figure 4(c) shows the transmission at the frequency of the single-cavity resonance. The noise pixels appear in this image, as expected, because they are isolated cavities. The pixels at the ends of the number 7 also showed a small amount of transmission at both frequencies. The end pixels have only one nearest neighbor that is altered, so their transmission spectrum appears slightly different from the other pixels in the image.

We also attempted to use this technique to remove salt noise, or white spots on a black background. We did this using an entire array of altered cavities and several isolated unaltered cavities. The band structure of this array is the lower set of solid curves in Fig. 2, which is shifted downward because the bulk of the array was altered with an extra acrylic layer. The single unaltered cavity with its higher resonant frequency attempts to create a defect state above the bottom of the energy band. However, states already exist at this higher frequency since the energy band of the lattice extends upward. These higher states are waves with large lateral wave vectors traveling in the bulk of the lattice. As a result there is strong coupling between the mode of the isolated, unaltered cavity and the bulk. The mode therefore has a low Q factor and is not detected in transmission measurements. This represents an interesting asymmetry between the two types of cavities.

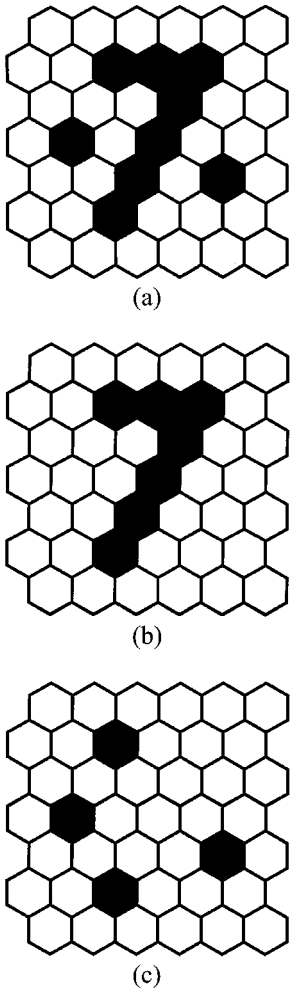

Fig. 4. (a) Original image of a number 7 with pepper noise. Black shading indicates which cavities have been altered with an extra layer of acrylic. (b) The nearest-neighbor AND function has removed the pepper noise, leaving the image of the number 7 intact. Black pixels are those with a transmission of more than -12 dB within a narrow frequency range. (c) Measuring at a higher frequency allows one to detect the single-cavity resonance associated with pepper noise. The end points of the number 7 also have some transmission at this frequency.

In conclusion, we have presented the 2-D band structure of a triangular array of vertical cavities. We have introduced defects into the lattice in the form of cavities that were altered by a slight increase in the dielectric constant to produce a downward shift in the resonant frequency. We have shown that these defects produce localized states below the energy band of the lattice. Furthermore, we have found that these altered cavities interact with each other to produce nonlinear Boolean logic functions. Specifically, nearest-neighbor AND, OR, and XOR functions have been described. Finally, we have demonstrated an important image-processing transformation by removing pepper noise from a sample image. We have also found an interesting asymmetry between low-frequency altered cavities and higher-frequency unaltered cavities, owing to the relative locations of the energy band and the defect state involved. The vertical-cavity array has been shown to be a useful image-processing element that can produce nonlinear logic functions with the inherent speed and parallelism of optical image-processing systems.

This research was supported by the U.S. Army Research Office under contract DAAH04-93-G-0227, the National Science Foundation under contract ECS-9307088, and the U.S. Air Force Office of Scientific Research under contract F49620-95-0534.

References

1. J. W. Goodman, *Introduction to Fourier Optics* (McGraw-Hill, New York, 1986).
2. S. H. Lee, ed., *Optical Information Processing Fundamentals* (Springer-Verlag, New York, 1981).
3. E. Yablonovitch, "Inhibited spontaneous emission in solid-state physics and electronics," Phys. Rev. Lett. **58,** 2059–2062 (1987).
4. S. John, "Strong localization of photons in certain disordered dielectric superlattices," Phys. Rev. Lett. **58,** 2486–2489 (1987).
5. J. D. Joanopolous, R. D. Meade, and Joshua N. Winn, *Photonic Crystals* (Princeton University Press, Princeton, 1995).
6. P. L. Gourley, M. E. Warren, G. A. Vawter, T. M. Brennan, and B. E. Hammons, "Optical Bloch waves in a semiconductor photonic lattice," Appl. Phys. Lett. **60,** 2714–2716 (1992).
7. T. A. Birks, P. J. Roberts, P. St. J. Russel, D. M. Atkin, and T. S. Shepherd, "Full 2-D photonic bandgaps in silica/air structures," Electron Lett. **31,** 1941–1943 (1995).
8. D. F. Sievenpiper, M. E. Sickmiller, and E. Yablonovitch, "3D wire mesh photonic crystals," Phys. Rev. Lett. **76,** 2480–2483 (1996).
9. N. W. Ashcroft and N. D. Mermin, *Solid State Physics* (Saunders College Publishing, New York, 1976).
10. P. W. Anderson, "The concept of frustration in spin glasses," J. Less Common Met. **63,** 291–294 (1978).
11. T.-H. Chao, "Dynamically reconfigurable optical morphological processor and its application," in *Optical Information Processing Systems and Architectures 4*, B. Javidi, ed., Proc. SPIE **1772,** 21–29 (1992).